

Biocompatibility of NeoPUTTY™ versus TheraCal PT® and TheraCal LC® pulp-capping materials, and tissue reaction following subcutaneous implantation in rats: Histological and molecular investigation

Dina Rady^{1,2,A–F}, Sara El Moshy^{1,2,A–F}, Yasmin Mohamed Yousry^{3,A–F}, Mohamed Ramadan^{4,A–F}, Israa Ahmed Radwan^{1,2,A–F}

¹ Department of Oral Biology, Faculty of Dentistry, Cairo University, Giza, Egypt

² Stem Cells and Tissue Engineering Research Group, Faculty of Dentistry, Cairo University, Giza, Egypt

³ Department of Pediatric Dentistry and Dental Public Health, Faculty of Dentistry, Cairo University, Giza, Egypt

⁴ Specialized Dental Hospital, Armed Forces Medical Complex, Cairo, Egypt

A – research concept and design; B – collection and/or assembly of data; C – data analysis and interpretation;

D – writing the article; E – critical revision of the article; F – final approval of the article

Dental and Medical Problems, ISSN 1644-387X (print), ISSN 2300-9020 (online)

Dent Med Probl. 2026;63(1):131–143

Address for correspondence

Sara El Moshy

E-mail: sarah.mahmoud@dentistry.cu.edu.eg

Funding sources

None declared

Conflict of interest

None declared

Acknowledgements

None declared

Received on April 20, 2023

Reviewed on June 7, 2023

Accepted on June 21, 2023

Published online on February 27, 2026

Cite as

Rady D, El Moshy S, Yousry YM, Ramadan M, Radwan IA. Biocompatibility of NeoPUTTY™ versus TheraCal PT® and TheraCal LC® pulp-capping materials, and tissue reaction following subcutaneous implantation in rats: Histological and molecular investigation. *Dent Med Probl.* 2026;63(1):131–143. doi:10.17219/dmp/168627

DOI

10.17219/dmp/168627

Copyright

Copyright by Author(s)

This is an article distributed under the terms of the Creative Commons Attribution 3.0 Unported License (CC BY 3.0) (<https://creativecommons.org/licenses/by/3.0/>).

Abstract

Background. Materials used for vital pulp therapy should support the natural healing and regeneration of the dental pulp. Ideally, these materials should be biocompatible, bioactive, non-toxic, and non-carcinogenic. Although numerous medicaments are currently available on the market, none fully meet all the criteria required for an ideal material. In recent years, calcium silicate-based materials, known for their bioactivity and biocompatibility, have gained widespread use in dental practice.

Objectives. This in vivo study investigated the tissue response and biological characteristics of mineral trioxide aggregate (MTA) – NeoPUTTY™, as well as TheraCal PT® and TheraCal LC®, following subcutaneous implantation in rats.

Material and methods. Twenty adult male albino rats were randomly assigned according to the sacrifice time (2 or 4 weeks) into 2 equal groups, which were further subdivided into 4 subgroups based on the material used. Four incisions were made on the back of each rat to create 4 pockets, into which polyethylene tubes were implanted. Three tubes were filled with biomaterials, while the 4th was left empty as a control. After sacrifice, the samples were analyzed histopathologically, histomorphometrically, and for gene expression of vascular endothelial growth factor (VEGF) and interleukin-6 (IL-6).

Results. Moderate inflammation was the predominant tissue response to NeoPUTTY. TheraCal LC demonstrated the formation of a thick connective tissue capsule with moderate chronic inflammatory cell infiltration. In contrast, TheraCal PT showed a mild inflammatory response and a lower area percentage of collagen fibers in the capsule as compared to NeoPUTTY and TheraCal LC. NeoPUTTY and TheraCal LC were associated with higher VEGF and IL-6 expression levels than those observed in the TheraCal PT and control groups.

Conclusions. TheraCal PT appears to be a promising material for direct pulp capping, owing to its favorable biocompatibility when tested in vivo in comparison with NeoPUTTY and TheraCal LC. These findings may assist clinicians in selecting appropriate materials for direct pulp capping, as TheraCal PT demonstrated greater biocompatibility with respect to its effects on the surrounding tissues.

Keywords: biocompatibility, subcutaneous tissue, TheraCal LC®, TheraCal PT®, NeoPUTTY™

Highlights

- Vital pulp therapy materials should promote pulp healing and regeneration.
- Calcium silicate-based materials are widely used due to their bioactivity and biocompatibility.
- TheraCal PT demonstrated superior *in vivo* biocompatibility in comparison with NeoPUTTY (mineral trioxide aggregate – MTA) and TheraCal LC.
- TheraCal PT shows potential as a promising material for direct pulp capping.
- Further studies are required to evaluate additional properties before clinical application.

Introduction

Dental caries in children is one of the most prevalent chronic degenerative diseases worldwide.¹ Its progression may result in irreversible damage to the dental pulp, potentially leading to the premature loss of deciduous or permanent teeth. One of the primary goals of pediatric dentistry is to maintain deciduous teeth in an intact and functional state until the eruption of their permanent successors.² Vital pulp therapy is commonly used treatment aimed at maintaining the vitality of carious teeth and preserving the health of the supporting tissues, thereby allowing deciduous or permanent teeth to be retained for as long as possible.³

Ideally, a pulp-capping material should promote the natural healing and regeneration of the dental pulp. It should be biocompatible, bioactive, non-toxic, and non-carcinogenic. In addition, it should exhibit adequate sealing ability, dimensional stability, an appropriate setting time, and good handling characteristics. Although numerous medicaments are currently available on the market, none fully meet all the criteria required for an ideal pulp-capping material.⁴ In recent years, calcium silicate-based materials, known for their bioactivity and biocompatibility, have gained widespread use in pediatric dental practice.⁵

Mineral trioxide aggregate (MTA) is one of calcium silicate-based materials that has been used in clinical practice for more than 2 decades. It has demonstrated high clinical effectiveness as a pulp-capping material owing to its excellent sealing ability, biocompatibility, and bioinductive and regenerative properties.⁶ Despite these advantages, MTA has several drawbacks, including a long setting time, poor handling characteristics, high solubility, potential for tooth discoloration, and relatively high cost.⁷ Consequently, several other calcium silicate-based materials have been developed to overcome these limitations while maintaining the favorable properties of MTA.

TheraCal LC[®] is a light-cured, resin-modified, calcium silicate-based cement. It has been reported to stimulate hydroxyapatite precipitation and dentin bridge formation.⁸ The material is supplied in a syringe, eliminating the need for mixing and simplifying handling. As compared to MTA, TheraCal LC exhibits lower solubility.⁹ Its

polymerization is associated with minimal heat generation, which may reduce adverse pulpal effects when used as a pulp-capping material. However, the presence of resin components that may remain partially unpolymerized could potentially have adverse effects on the pulpal tissue, particularly as its interaction with the pulp has not been extensively investigated.¹⁰

TheraCal PT[®] is a newer calcium silicate-based material; it is a dual-cured, resin-modified cement. It was introduced as a biocompatible material intended to maintain tooth vitality by acting as a protective barrier for the dental pulp. Similar to TheraCal LC, it is supplied in a syringe, eliminating the need for mixing, and is characterized by low solubility and a short setting time. In addition, its dual-curing capability represents a potential advantage over TheraCal LC, as it enables its use in procedures such as pulpotomy in primary molars. However, there is still limited evidence regarding its effectiveness and biocompatibility.¹¹

NeoPUTTY[™] is a new pre-mixed, bioactive, bioceramic, calcium silicate-based material. According to the manufacturer, this multipurpose MTA stimulates hydroxyapatite formation, promoting bioactivity and supporting tissue healing. NeoPUTTY is dimensionally stable with no shrinkage, providing a reliable seal and minimizing bacterial infiltration. Unlike conventional MTA, it exhibits immediate washout resistance, allowing the final restoration and crown cementation to be performed immediately after placement.¹² The putty-like material is supplied in a syringe with a plunger tip, enabling easy and rapid application while minimizing waste and reducing cost. Additionally, NeoPUTTY has no staining potential, since tantalum oxide is used for radiopacity instead of bismuth oxide, the primary cause of tooth discoloration associated with MTA. Being resin-free, the material may also have enhanced biocompatibility and bioactivity.¹²

In general, newly developed materials with modified composition should be thoroughly evaluated before clinical use. Given the lack of data on the interaction of NeoPUTTY with the pulpal tissue, and limited information available for TheraCal PT and TheraCal LC, this study aimed to investigate the *in vivo* biocompatibility of TheraCal PT, TheraCal LC and NeoPUTTY, following subcutaneous implantation in rats.

Material and methods

The pulp-capping materials used in the study were as follows: TheraCal PT (ThPT; BISCO, Schaumburg, USA); TheraCal LC (ThLC; BISCO) and NeoPUTTY (NPU; Avalon Biomed, Houston, USA). The composition of the materials is described in Table 1.

Study design and animals

According to the guidance and approval of the Institutional Animal Care and Use Committee of Cairo University (CU-IACUC), this experiment was conducted in the animal house of the Faculty of Medicine, Cairo University, Giza, Egypt, in accordance with the ARRIVE guidelines for in vivo animal research. Twenty adult male albino rats weighing 150–200 g were obtained from the animal house. The animals were housed in temperature-controlled rooms, and provided with food and water ad libitum. The care and maintenance of the experimental animals conformed to the International Guiding Principles for Biomedical Research Involving Animals. The rats were randomly divided into 2 groups ($n = 10$ per group) according to the sacrifice time points – 2 weeks and 4 weeks. These groups were further subdivided into 4 subgroups according to the material used (Table 2).

Sample size

According to a previous study,¹³ a total sample of 20 rats (10 rats per group) was considered sufficient to detect an effect size of 1.23 with a statistical power of 0.80, using a two-sided hypothesis test and a significance level (α) of 0.05. The sample size was calculated using the G*power program (<https://www.psychologie.hhu.de/arbeitsgruppen/allgemeine-psychologie-und-arbeitspsychologie/gpower>).¹⁴

Sample preparation

The 3 test materials were placed in sterile polyethylene tubes. TheraCal PT and TheraCal LC were light-cured for 20 s, using a light-curing unit (PenCure, J. Morita, Kyoto, Japan).

Anesthesia and the surgical protocol

The animals were anesthetized with an intraperitoneal injection of ketamine (80 mg/kg of body weight (b.w.)) and xylazine hydrochloride (8 mg/kg b.w.). The back of each animal was shaved and disinfected with 10% betadine antiseptic solution (Mundipharma Egypt, Cairo, Egypt). Four incisions, 2 cm in length, were made on the back of each rat to create 4 pockets, into which polyethylene

Table 1. Pulp-capping materials used in the study

Commercial name	Manufacturer	Composition	Lot #
TheraCal PT	BISCO, Schaumburg, USA	synthetic Portland cement calcium silicate particles in a hydrophilic matrix	2000004394
TheraCal LC	BISCO, Schaumburg, USA	tricalcium silicate particles in a hydrophilic monomer	2000004742
NeoPUTTY	Avalon Biomed, Houston, USA	inorganic powder of tricalcium/dicalcium silicate in an organic medium	2020070101

Table 2. Study grouping

Groups	Sacrifice time	Subgroups	
Group 1 ($n = 10$)	2 weeks	MTA subgroup 1	polyethylene tubes filled with NeoPUTTY MTA ($n = 10$ tubes)
		TheraCal LC subgroup 1	polyethylene tubes filled with TheraCal LC ($n = 10$ tubes)
		TheraCal PT subgroup 1	polyethylene tubes filled with TheraCal PT ($n = 10$ tubes)
		control subgroup 1	empty polyethylene tubes (control) ($n = 10$ tubes)
Group 2 ($n = 10$)	4 weeks	MTA subgroup 2	polyethylene tubes filled with NeoPUTTY MTA ($n = 10$ tubes)
		TheraCal LC subgroup 2	polyethylene tubes filled with TheraCal LC ($n = 10$ tubes)
		TheraCal PT subgroup 2	polyethylene tubes filled with TheraCal PT ($n = 10$ tubes)
		control subgroup 2	empty polyethylene tubes (control) ($n = 10$ tubes)

MTA – mineral trioxide aggregate.

tubes were implanted. Three tubes were filled with the biomaterials under study, while the 4th was left empty as a negative control of the histological reaction. The tubes were placed with at least 2 cm distance between them to avoid interference in the tissue response. The skin was closed using 4/0 silk sutures (ISMC, Belbais, Egypt).

Postoperative care

Postoperatively, each animal received intramuscular injections of 10 mg/kg b.w. of amoxicillin and flucloxacillin (Flumox[®]; Eipico, 10th of Ramadan City, Egypt) to prevent secondary bacterial infection, and 10 mg/kg b.w. diclofenac potassium (Cataflam[®]; Novartis, Cairo, Egypt) for postoperative analgesia. In addition, a topical antibiotic spray containing neomycin (Bivatracin[®]; Egyptian Company for Advanced Pharmaceuticals, Cairo, Egypt) was applied to prevent local infection.

Animal sacrifice

The animals were euthanized by an intracardiac overdose of sodium thiopental (80 mg/kg b.w.) at 2 or 4 weeks after implantation, according to the experimental group.

Samples of skin and subcutaneous tissues containing the implants were excised with a safety margin of 1 cm. The tissues from one side of the tube interface were immediately fixed in 10% neutral buffered formalin for histopathological analysis. The tissues from the other side of the tube interface were frozen in liquid nitrogen and stored at -70°C for subsequent RNA extraction and gene expression analysis.¹⁵

Histopathological and histomorphometric analysis

The formalin-fixed tissue samples were dehydrated using ascending grades of alcohol, and then embedded in paraffin wax. The paraffin blocks were sectioned into 5- μm -thick slices and stained with hematoxylin and eosin (H&E) and Masson's trichrome (MT).

The H&E-stained sections were examined and photographed using a light microscope equipped with a digital camera (Leica, Heerbrugg, Switzerland) at magnifications of $\times 10$, $\times 40$ and $\times 100$. The acquired images were analyzed using the ImageJ software, v. 1.53d (<https://imagej.net/ij>).¹⁶ All quantitative analyses were performed on all animals ($N = 20$). For each animal, 3 non-serial sections were examined for each material, and the mean value was calculated. Morphometric analyses were conducted by a single calibrated and blinded examiner.

Number and density of inflammatory cells

The number of inflammatory cells was estimated within the connective tissue capsules. For the detection

of inflammatory cell number and density, The H&E-stained sections were examined using a light microscope equipped with a digital camera (Leica) at $\times 40$ magnification. An image of a standardized field of the capsule in close proximity to the tube opening was captured.¹⁷ The acquired images were analyzed using the ImageJ software, v. 1.53d (<https://imagej.net/ij>).¹⁶ For each field, the total number of inflammatory cells, including neutrophils, lymphocytes, plasma cells, macrophages, and giant cells, was determined. The density of inflammatory cells (the number of cells per square millimeter of the capsule) was then calculated by dividing the total number of inflammatory cells by the total area of the capsule field, as previously described.^{17–19}

Grade of connective tissue capsule inflammation

According to the number of inflammatory cells, the inflammatory reaction was graded as follows: Grade 0 – no inflammatory cells detected; Grade 1 – fewer than 25 cells detected; Grade 2 – 25–125 cells detected; and Grade 3 – more than 125 cells detected.^{20,21}

Grade of inflammation extension

The histological images were also graded according to the extent of inflammatory cell spread within the connective tissue capsule and the surrounding connective tissue as follows: Grade 0 – no inflammatory cells detected; Grade 1 – inflammatory cells confined to the area of the capsule adjacent to the implanted tubes; Grade 2 – inflammatory cells restricted to the capsule without extension into the surrounding connective tissue; and Grade 3 – inflammatory cells extending beyond the capsule into the surrounding connective tissue.²²

Capsule thickness

For the evaluation of capsular thickness, the H&E-stained sections were examined using a light microscope equipped with a digital camera (Leica) at $\times 10$ magnification. The acquired images were analyzed using the ImageJ software, v. 1.53d (<https://imagej.net/ij>).¹⁶ The thickness of the central part of the capsule was measured in 3 non-serial sections, and the mean value was calculated for each material.¹⁹

Area percentage of collagen fibers within the capsule

The MT-stained sections were examined using a light microscope equipped with a digital camera (Leica) at $\times 40$ magnification. The acquired images were analyzed using the ImageJ software, v. 1.53d (<https://imagej.net/ij>).¹⁶ The area percentage of collagen fibers within the capsule was measured in the MT-stained sections using ImageJ, as previously described.²³

Quantitative real-time polymerase chain reaction (qRT-PCR) assays

Quantitative real-time polymerase chain reaction (qRT-PCR) assays were performed using a real-time thermal detection system with total RNA, the iScript™ one-step RT-PCR kit with SYBR® Green (Bio-Rad Laboratories, Hercules, USA), and specific primers. The gene-specific primer sequences used for amplification are listed in Table 3. β -actin was used as the internal control. Relative gene expression levels of vascular endothelial growth factor (VEGF) and interleukin-6 (IL-6) were quantified using the $2^{-\Delta\Delta CT}$ method.

Table 3. Primer sequences of all studied genes

Gene	Primer sequence from 5' to 3'
VEGF	forward: 5'-CACGACAGAAGGGGAGCAGAA-3'
	reverse: 5'-TGCGGATCTTGGACAAACAAAT-3'
IL-6	forward: 5'-TCCTACCCCAACTTCCAATGCTC-3'
	reverse: 5'-TTGGATGGTCTTGGTCTTAGCC-3'
β -actin	forward: 5'-GTGACATCCACCCAGAGG-3'
	reverse: 5'-ACAGGATGTCAAACCTGCC-3'

Statistical analysis

Data obtained from both the histomorphometric analysis and the RT-PCR assays, estimated at 2 and 4 weeks, was expressed as mean \pm standard deviation ($M \pm SD$). Normally distributed parametric data was analyzed using one-way or two-way analysis of variance (ANOVA) tests. Tukey's post hoc test was applied for multiple pairwise comparisons when the ANOVA results were statistically significant. Non-parametric data was analyzed using the Kruskal–Wallis test followed by Dunn's post hoc test for statistically significant results. A p -value <0.05 was considered statistically significant. Statistical analysis was performed using the Statistical Package for the Social Sciences (SPSS), v. 15.0 (SPSS Inc., Chicago, USA).

Results

Histopathological results

Group 1 (two-week interval)

H&E staining:

MTA subgroup 1 (Fig. 1A, 1B) and TheraCal LC subgroup 1 (Fig. 1C, 1D) revealed a thick connective tissue capsule with a moderate inflammatory reaction. The aggregations of chronic inflammatory cells were observed within the unorganized fibrous connective tissue containing numerous plasma cells and lymphocytes, along with some fibroblasts. Mineralization was observed in both groups (Fig. 1A, 1C). At higher magnification, congested

blood vessels were evident in the MTA subgroup 1 (Fig. 1B), while multinucleated giant cells were observed in the TheraCal LC subgroup 1 (Fig. 1D). TheraCal PT subgroup 1 exhibited a mild inflammatory reaction with a thinner capsule. The remnants of the implanted material were also observed (Fig. 1E, 1F). The control subgroup 1 showed more organized connective tissue with a mild inflammatory reaction and few lymphocytes (Fig. 1G, 1H). Fibroblasts were observed in all subgroups of group 1.

MT staining:

MTA subgroup 1 (Fig. 2A) and TheraCal LC subgroup 1 (Fig. 2B) revealed slightly stained, thin and irregularly arranged collagen fibers within the inflammatory capsule. TheraCal PT subgroup 1 showed prominent deposition of thin, irregular collagen fibers (Fig. 2C). The control sub-

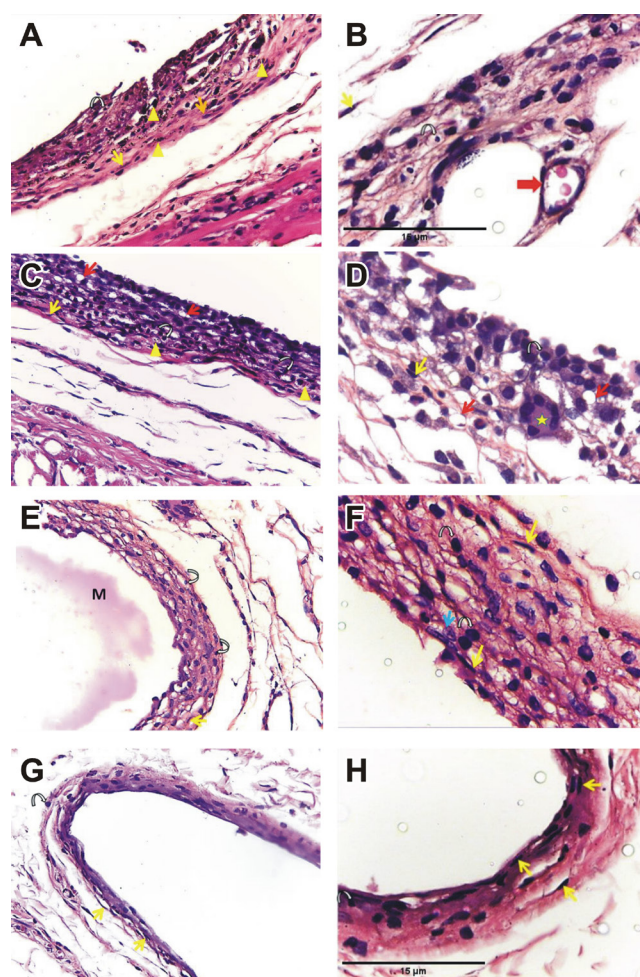


Fig. 1. Histopathological examination of the subcutaneous connective tissue responses to all the tested pulp-capping materials and the empty tube (control) in rats at 2 weeks (group 1); hematoxylin and eosin (H&E) staining A, B – MTA subgroup 1 (A – moderate inflammatory reaction, the tissue packed with inflammatory cells, with multiple areas of mineralization (triangle), B – congested blood vessels (red arrow)); C, D – TheraCal LC subgroup 1 (C – moderate inflammatory reaction, the tissue packed with inflammatory cells, with few areas of mineralization (triangle), D – multinucleated giant cells (yellow star)); E, F – TheraCal PT subgroup 1 (E – mild inflammatory reaction, remnants of the material (M), F – some inflammatory cells); G, H – control subgroup 1 (mild inflammatory reaction, inflammatory cells). Cells observed: white arrow – lymphocytes; yellow arrow – fibroblasts; blue arrow – plasma cells. A, C, E, G $\times 40$ magnification; B, D, F, H $\times 100$ magnification.

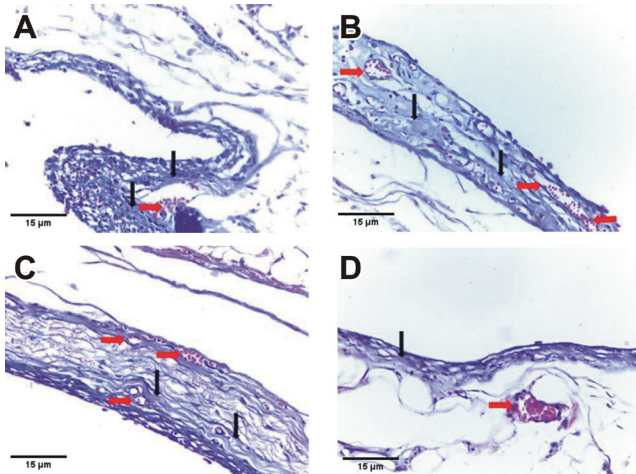


Fig. 2. Histopathological examination of the subcutaneous connective tissue responses to all the tested pulp-capping materials and the empty tube (control) in rats at 2 weeks (group 1); Masson's trichrome (MT) staining

A – MTA subgroup 1; B – TheraCal LC subgroup 1; C – TheraCal PT subgroup 1; D – control subgroup 1; slightly stained collagen in a meshwork arrangement (black arrow), associated with congested vessels (red arrow) in all subgroups (A–D). $\times 40$ magnification.

group 1 showed mild collagen fiber deposition (faint blue) with fibroblasts and a few capillaries (Fig. 2D). Congested blood vessels were observed in all subgroups of group 1.

Group 2 (four-week interval)

H&E staining:

MTA subgroup 2 revealed a relatively thick fibrous capsule with limited organization and mild peri-capsular fibrosis, along with some congested capillaries (Fig. 3A, 3B). TheraCal LC subgroup 2 showed disorganized reactionary tissue with edema between collagen fibers and scattered inflammatory cell infiltration (Fig. 3C, 3D). TheraCal PT subgroup 2 demonstrated a relatively organized fibrous capsule with several active fibroblasts characterized by swollen, large nuclei and abundant cytoplasm. A marked decrease in inflammatory cell infiltration with mild peri-capsular fibrosis was also observed (Fig. 3E, 3F). The control subgroup 2 exhibited uniform collagen fiber formation. Collagen fibers were thin and discrete, with mild inflammatory infiltrate, mainly represented by lymphocytes and interspersed fibroblasts (Fig. 3G, 3H).

MT staining:

MTA subgroup 2 (Fig. 4A) and TheraCal LC subgroup 2 (Fig. 4B) revealed several fibroblasts within a band of dense collagen fibers, which stained lighter with trichrome as compared to the collagen fibers observed in mature granulation tissue. Fibroblasts and blood vessels were also present, and inflammatory cells, mainly lymphocytes, were evident. TheraCal PT subgroup 2 (Fig. 4C) and the control subgroup 2 (Fig. 4D) showed deposition of regularly arranged collagen fibers, along with evidence of newly formed blood vessels.

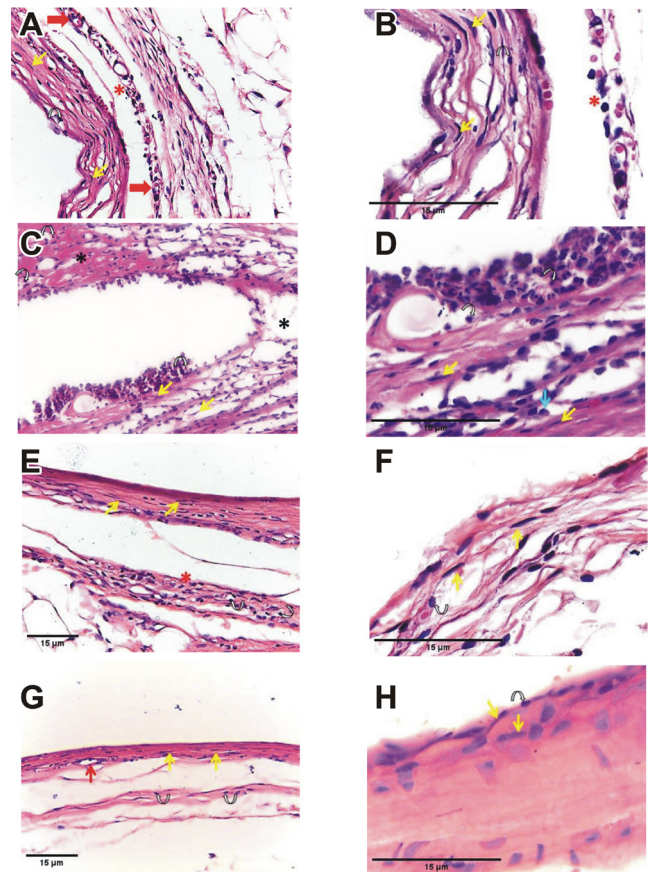


Fig. 3. Histopathological examination of the subcutaneous connective tissue responses to all the tested pulp-capping materials and the empty tube (control) in rats at 4 weeks (group 2); hematoxylin and eosin (H&E) staining

A, B – MTA subgroup 2 (A – mild inflammatory reaction with some inflammatory cells and congested capillaries (red arrow), B – mild peri-capsular fibrosis (red asterisk)); C, D – TheraCal LC subgroup 2 (C – disorganized reactionary tissue with edema (black asterisk), D – chronic inflammatory cell infiltrate); E, F – TheraCal PT subgroup 2 (E – well-organized reactionary tissue with dense collagen fibers, occasionally infiltrated by lymphocytes, F – active fibroblasts); G, H – control subgroup 2 (thin reactionary tissue with organized collagen fibers, fibroblasts and a mild inflammatory reaction). Cells observed: white arrow – lymphocytes; yellow arrow – fibroblasts; blue arrow – plasma cells. A, C, E, G $\times 40$ magnification; B, D, F, H $\times 100$ magnification.

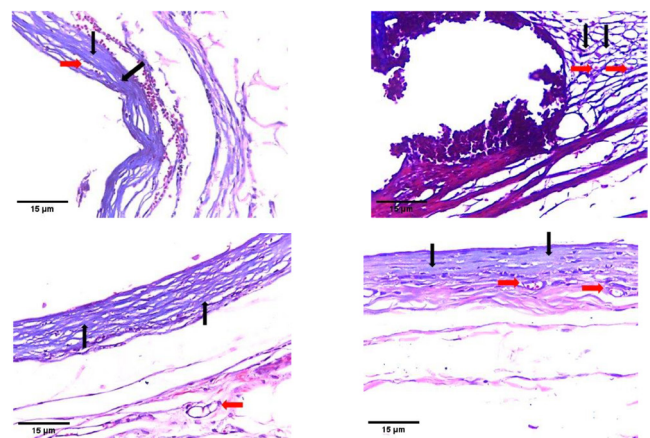


Fig. 4. Histopathological examination of the subcutaneous connective tissue responses to all the tested pulp-capping materials and the empty tube (control) in rats at 4 weeks (group 2); Masson's trichrome (MT) staining

A – MTA subgroup 2; B – TheraCal LC subgroup 2; C – TheraCal PT subgroup 2; D – control subgroup 2; collagen fibers forming a mesh (black arrow) amongst inflammatory cells, blood vessels (red arrow) in all subgroups (A–D). $\times 40$ magnification.

Number and density of inflammatory cells

Statistically significantly lower mean values for both the number and density of inflammatory cells were recorded in the control subgroup, followed by the TheraCal PT subgroup, as compared to the TheraCal LC and MTA subgroups at both observational time points (group 1 and group 2). No significant difference was found between the TheraCal LC and MTA subgroups at either time point. A statistically significant time-dependent decrease in the number and density of inflammatory cells was observed in the TheraCal PT, TheraCal LC and MTA subgroups (Table 4, Fig. 5A, 5B, Supplementary Table 1).

Capsule thickness

A statistically significantly lower mean value of the capsule thickness was recorded in the control subgroup, followed by the TheraCal PT subgroup, as compared to the TheraCal LC and MTA subgroups at both observational time points (group 1 and group 2). No significant difference was found between the TheraCal LC and MTA subgroups at either time point. A statistically significant time-dependent increase in the capsule thickness was observed in all subgroups (Table 4, Fig. 5C, Supplementary Table 1).

Table 4. Two-way ANOVA results for the number and density of inflammatory cells, the capsule thickness, and the area percentage of collagen fibers within the capsule

Parameter	Group	Subgroup	$M \pm SD$	SE	F	p-value		
Number of inflammatory cells (n)	group 1	MTA subgroup 1	90.4 ± 29.7 ^A	9.39	7.27	0.000*		
		TheraCal LC subgroup 1	92.0 ± 33.8 ^A	10.70				
		TheraCal PT subgroup 1	46.5 ± 14.2 ^B	4.49				
		control subgroup 1	18.8 ± 6.6 ^{CD}	2.07				
	group 2	MTA subgroup 2	36.1 ± 1.7 ^{BC}	0.53				
		TheraCal LC subgroup 2	38.4 ± 7.2 ^{BC}	2.26				
		TheraCal PT subgroup 2	12.0 ± 3.2 ^D	1.01				
		control subgroup 2	8.3 ± 2.5 ^D	0.80				
Density of inflammatory cells [n/mm ²]	group 1	MTA subgroup 1	0.973 ± 0.320 ^A	0.101	4.09	0.000*		
		TheraCal LC subgroup 1	0.991 ± 0.364 ^A	0.115				
		TheraCal PT subgroup 1	0.501 ± 0.153 ^B	0.048				
		control subgroup 1	0.202 ± 0.071 ^{CD}	0.022				
	group 2	MTA subgroup 2	0.388 ± 0.018 ^{BC}	0.006				
		TheraCal LC subgroup 2	0.414 ± 0.077 ^{BC}	0.024				
		TheraCal PT subgroup 2	0.129 ± 0.034 ^D	0.011				
		control subgroup 2	0.089 ± 0.027 ^D	0.009				
Capsule thickness [mm]	group 1	MTA subgroup 1	20.68 ± 6.31 ^{BC}	2.00	4.09	0.010*		
		TheraCal LC subgroup 1	26.03 ± 4.19 ^B	1.32				
		TheraCal PT subgroup 1	11.43 ± 2.60 ^D	0.82				
		control subgroup 1	5.20 ± 1.27 ^E	0.40				
	group 2	MTA subgroup 2	38.06 ± 6.00 ^A	1.90				
		TheraCal LC subgroup 2	42.51 ± 5.40 ^A	1.71				
		TheraCal PT subgroup 2	21.59 ± 1.80 ^{BC}	0.57				
		control subgroup 2	15.89 ± 2.34 ^{CD}	0.74				
Area percentage of collagen fibers within the capsule [%]	group 1	MTA subgroup 1	55.85 ± 3.76 ^{AB}	1.19	16.75	0.000*		
		TheraCal LC subgroup 1	63.06 ± 7.26 ^A	2.30				
		TheraCal PT subgroup 1	50.20 ± 9.43 ^{BC}	2.98				
		control subgroup 1	42.32 ± 1.68 ^C	1.68				
	group 2	MTA subgroup 2	68.66 ± 4.79 ^A	1.52			26.03	0.000*
		TheraCal LC subgroup 2	73.05 ± 5.87 ^A	1.86				
		TheraCal PT subgroup 2	60.74 ± 9.27 ^B	2.93				
		control subgroup 2	50.70 ± 2.18 ^C	0.69				

M – mean; SD – standard deviation; SE – standard error; * statistically significant; means with different superscript letters are significantly different.

Area percentage of collagen fibers within the capsule (MT stain)

Two-way ANOVA revealed no significant interaction between treatment and time, while a significant difference was detected among the different kinds of treatment within each time period. Therefore, one-way ANOVA was used to compare the subgroups at each time point.

One-way ANOVA for the 2-week subgroups showed a statistically significantly lower mean value in the control subgroup 1, followed by the TheraCal PT subgroup 1, as compared to the TheraCal LC and MTA subgroups 1. Similarly, one-way ANOVA for the 4-week subgroups demonstrated a statistically significantly lower mean value in the control subgroup 2, followed by the TheraCal PT subgroup 2. No statistically significant difference was found between the TheraCal LC and MTA subgroups at either observational time point (group 1 and group 2) (Table 4, Fig. 6, Supplementary Table 1).

Grade of connective tissue capsule inflammation and the grade of inflammation spread into the adjacent connective tissue

Regarding group 1 (2-week time point), most specimens in the control subgroup 1 exhibited Grade 1 connective tissue capsule inflammation, whereas the majority of specimens in the TheraCal PT, TheraCal LC and MTA subgroups 1 showed Grade 2 inflammation. A statistically significantly lower value was observed in the control subgroup 1 as compared to the other groups, while no statistically significant difference was found among the TheraCal PT, TheraCal LC and MTA subgroups 1. At the 4-week time point (group 2), all specimens in the control subgroup 2 and the TheraCal PT subgroup 2 exhibited Grade 1 inflammation. The majority of specimens in the TheraCal LC subgroup 2 showed Grade 2 inflammation, whereas half of the specimens in the MTA subgroup 2 exhibited Grade 1 inflammation and the other half showed

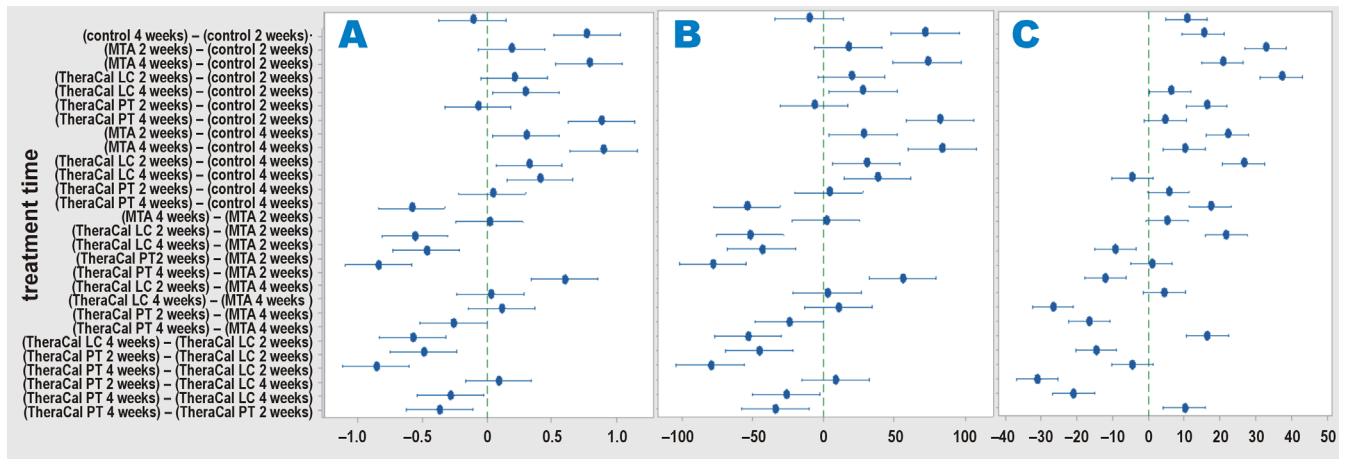


Fig. 5. Tukey's post hoc test results

A – density of inflammatory cells; B – number of inflammatory cells; C – capsule thickness.

95% confidence interval (CI). If an interval does not contain zero, the corresponding means are significantly different.

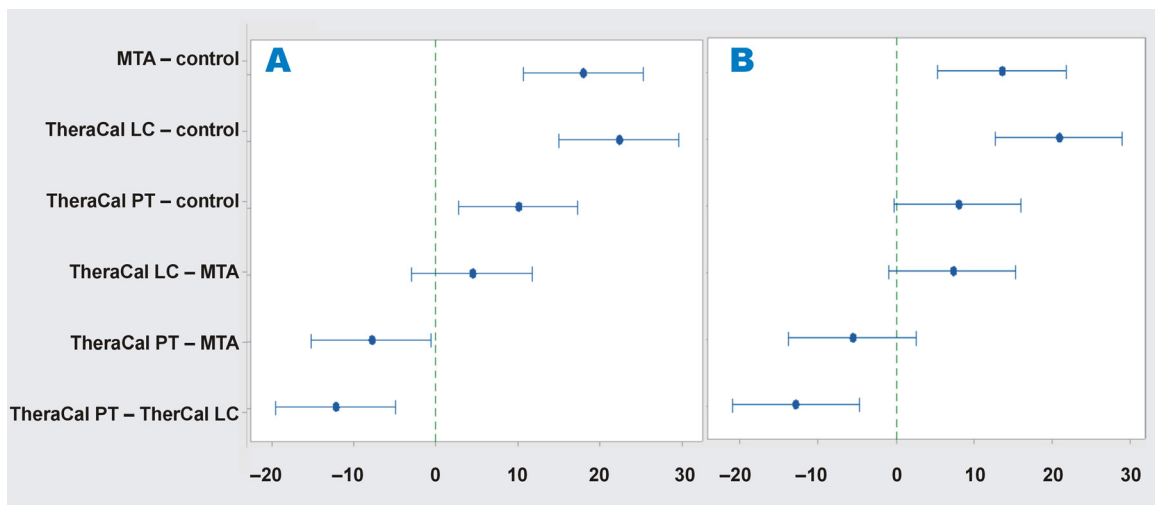


Fig. 6. Tukey's post hoc test results for the area percentage of collagen fibers within the capsule

A – at 2 weeks; B – at 4 weeks.

95% CI. If an interval does not contain zero, the corresponding means are significantly different.

Table 5. Kruskal–Wallis test results for the grade of connective tissue capsule inflammation and the grade of inflammation spread into the adjacent connective tissue

Parameter	Group	Subgroup	Grade (n)			p-value
			G1	G2	G3	
Grade of connective tissue capsule inflammation	group 1	MTA subgroup 1 ^A	0	9	1	0.000*
		TheraCal LC subgroup 1 ^A	0	8	2	
		TheraCal PT subgroup 1 ^A	0	10	0	
	group 2	control subgroup 1 ^B	8	2	0	0.001*
		MTA subgroup 2 ^A	5	5	0	
		TheraCal LC subgroup 2 ^A	3	7	0	
		TheraCal PT subgroup 2 ^B	10	0	0	
Grade of inflammation spread into the adjacent connective tissue	group 1	control subgroup 2 ^B	10	0	0	0.000*
		MTA subgroup 1 ^A	4	1	5	
		TheraCal LC subgroup 1 ^A	1	0	9	
	group 2	TheraCal PT subgroup 1 ^B	8	2	0	0.000*
		control subgroup 1 ^B	8	2	0	
		MTA subgroup 2 ^A	0	5	5	
		TheraCal LC subgroup 2 ^A	0	3	7	
group 2	TheraCal PT subgroup 2 ^B	8	1	1	0.000*	
	control subgroup 2 ^B	9	0	1		

* statistically significant; means with different superscript letters are significantly different.

Grade 2 inflammation. The differences between the TheraCal PT subgroup 2 and both the TheraCal LC subgroup 2 and the MTA subgroup 2 were statistically significant, while the difference between the MTA and TheraCal LC subgroups 2 was not statistically significant (Table 5, Supplementary Table 2).

At both observational time points, most specimens in the control and TheraCal PT subgroups exhibited Grade 1 inflammation spread into the adjacent connective tissue, whereas most specimens in the TheraCal LC and MTA subgroups exhibited Grade 3. The differences between the TheraCal PT subgroup and both the TheraCal LC and MTA subgroups were statistically significant, while the difference between the MTA and TheraCal LC subgroups was not statistically significant at either observational time point (group 1 and group 2) (Table 5, Supplementary Table 2).

A statistically significant decrease in both the grade of inflammation and the grade of inflammation spread into the adjacent connective tissue was observed over time in all subgroups (Table 5, Supplementary Table 2).

Quantitative RT-PCR analysis

Regarding the VEGF mRNA gene expression levels, statistical analysis demonstrated a statistically significantly lower mean value in the TheraCal PT subgroup as compared to the TheraCal LC and MTA subgroups at both observational time points. A statistically significant lower value was also detected in the MTA subgroup as compared to the TheraCal LC subgroup. A statistically

significant decrease in VEGF gene expression over time was observed in the TheraCal PT and TheraCal LC subgroups (Table 6, Fig. 7, Supplementary Table 3).

Statistical analysis of mRNA gene expression of IL-6 revealed a statistically significantly lower mean value in the TheraCal PT subgroup as compared to both the TheraCal LC and MTA subgroups, while no significant difference was detected between the TheraCal LC and MTA subgroups at either observational time point. A statistically significant decrease in IL-6 gene expression was observed for all 3 materials over time (Table 6, Fig. 7, Supplementary Table 3).

Discussion

Vital pulp therapy is a promising individualized treatment approach for managing irreversible pulpitis and promoting dentin bridge formation. Biocompatibility is an essential characteristic that must be considered in the case of the materials applied directly to the exposed pulp tissue.²⁴ Materials intended for direct pulp capping should be non-cytotoxic to dental pulp stem cells and bioactive in promoting odontogenic differentiation. However, in vitro cell culture assays cannot fully predict in vivo tissue responses. Therefore, in addition to cytotoxicity tests, animal studies and clinical evaluations are necessary to safeguard against the potential adverse effects of newly introduced dental materials.²⁵

Subcutaneous implantation in vivo is considered one of the most reliable methods for assessing the

Table 6. Two-way ANOVA results for vascular endothelial growth factor (VEGF) and interleukin-6 (IL-6) gene expression

Gene expression	Group	Subgroup	$M \pm SD$	SE	F	p-value
VEGF	group 1 ^A	MTA subgroup 1	0.3757 ± 0.0723 ^D	0.0229	4.33	0.007*
		TheraCal LC subgroup 1	0.6205 ± 0.0515 ^B	0.0107		
		TheraCal PT subgroup 1	0.3015 ± 0.0339 ^E	0.0163		
		control subgroup 1	1 ^A	0		
	group 2 ^B	MTA subgroup 2	0.3492 ± 0.0282 ^{DE}	0.0089		
		TheraCal LC subgroup 2	0.5475 ± 0.0309 ^C	0.0124		
		TheraCal PT subgroup 2	0.2271 ± 0.0394 ^F	0.0098		
IL-6	group 1 ^A	MTA subgroup 1	0.37 ± 0.01 ^B	0.003	15.43	0.000*
		TheraCal LC subgroup 1	0.38 ± 0.05 ^B	0.015		
		TheraCal PT subgroup 1	0.29 ± 0.03 ^C	0.008		
		control subgroup 1	1 ^A	0		
	group 2 ^B	MTA subgroup 2	0.27 ± 0.03 ^C	0.010		
		TheraCal LC subgroup 2	0.29 ± 0.03 ^C	0.009		
		TheraCal PT subgroup 2	0.22 ± 0.02 ^D	0.007		
		control subgroup 2	1 ^A	0		

* statistically significant; means with different superscript letters are significantly different.

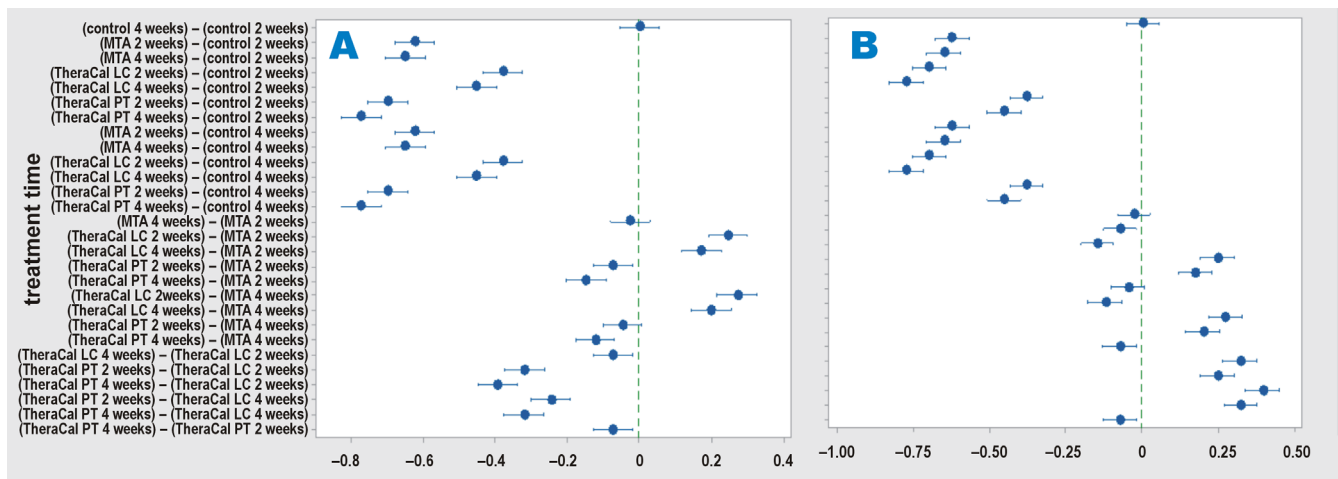


Fig. 7. Dot plot showing Tukey's post hoc test results for gene expression

A – vascular endothelial growth factor (VEGF); B – interleukin-6 (IL-6).

95% CI. If an interval does not contain zero, the corresponding means are significantly different.

biocompatibility of dental materials.^{26,27} Based on this concept, the present study aimed to evaluate the biological characteristics of MTA (NeoPUTTY), TheraCal LC and TheraCal PT, following subcutaneous implantation in rats.

The pulp-capping material extruded from the opening of the polyethylene tube comes into direct contact with the surrounding tissues, triggering an inflammatory response similar to that observed in vital pulp therapy. Inert polyethylene tubes were used for implantation, since they allow the tested material to remain in close apposition to the tissues.²⁶ An additional empty tube was implanted as a control to standardize variables, minimize selection bias, and neutralize the potential confounding factors that

could affect the results.²⁸ The follow-up periods were set at 2 and 4 weeks, following Silva-Herzog et al., who reported that 14 days are sufficient to evaluate the initial phase of material biocompatibility.²⁹

At 2 weeks, the inflammatory responses observed in the control subgroup 1 and in all the evaluated materials (NeoPUTTY, TheraCal LC and TheraCal PT) were more pronounced than those observed at 4 weeks. In addition to the potential toxic effects of the implanted materials and the tube material, the surgical trauma induced during tube insertion might also contribute to this response.³⁰ Giraud et al. suggested that there exists a dynamic equilibrium between inflammation and regeneration, and

that this balance may shift toward either regeneration or inflammation, depending on the restorative material used.³¹

Moderate inflammation was the characteristic tissue response to MTA, which decreased after 4 weeks of exposure to the material. These findings are consistent with those of Shahi et al., who reported the presence of collagen fibers, fibrosis and persistent inflammatory cell infiltration after 21 days.³² Inflammation may result from multiple factors; however, the initial inflammatory response can be triggered by factors such as cytokine production (e.g., IL-1 and IL-6), as well as the high pH and setting temperature of the material.³³ The formation of calcium deposits in the subcutaneous connective tissue indicates the osteoinductive potential of the tested material.³⁴ The mineralization observed in the MTA subgroup may be attributed to the reaction between calcium ions from calcium hydroxide and carbon dioxide present in the connective tissue. Calcium hydroxide is formed from calcium phosphate and calcium oxide released during the setting reaction of MTA.³²

The histological examination and histomorphometric analysis of the TheraCal LC subgroup 1 demonstrated the presence of a thick connective tissue capsule with moderate aggregations of chronic inflammatory cells. The resin component of TheraCal LC may lead to the release of residual monomers, which can diffuse into the surrounding tissues, exert cytotoxic effects and stimulate the production of pro-inflammatory cytokines.³¹ It has been suggested that TheraCal LC may shift the biological balance toward inflammation, whereas resin-free materials tend to exhibit anti-inflammatory properties and promote tissue regeneration.²⁴ Similarly, the histological examination of TheraCal LC used in primary teeth with deep carious lesions and symptoms of reversible pulpitis revealed the disruption of the odontoblastic layer, fibrosis and dystrophic calcification, along with varying degrees of pulpitis in the examined specimens, indicating that none of the samples presented completely healthy pulp tissue.³⁵

In addition to Portland cement powder, TheraCal LC contains a hydrophilic resin monomer, a hydrophobic resin monomer and a hydrophilic fillers.³⁶ Methacrylate resin components can adversely affect cell membranes by disrupting the lipid bilayer. Previous studies have demonstrated that the exposure of human dental pulp stem cells to TheraCal LC results in impaired cellular metabolism and the formation of inadequate tissue bridges.^{37,38} Furthermore, the cells cultured in the media containing TheraCal LC exhibit markedly elevated levels of IL-8.³⁹ Evidence of mineralization was observed in the TheraCal LC subgroup, which is consistent with the findings of Hinata et al., who evaluated the ability of TheraCal LC to form apatite-like precipitates at 7, 14, and 28 days after subcutaneous implantation in rats.⁴⁰ Although TheraCal LC has been reported not to produce calcium hydroxide during hydration, calcium ion release and calcium

phosphate deposition have been detected on its surface.³⁶ This phenomenon may be attributed to the resin-modified nature of TheraCal LC, which limits ion exchange with the surrounding environment. Consequently, the water absorption and calcium ion release associated with cement hydration may be restricted due to limited ion transport across and within the resin matrix.

The TheraCal PT subgroup demonstrated a mild inflammatory response that decreased over time, along with a lower percentage area of collagen fibers within the fibrous capsule as compared to the MTA and TheraCal LC subgroups. These findings suggest that TheraCal PT exhibits a lower cytotoxic effect on the surrounding tissues. The present results are consistent with those reported by Rodríguez-Lozano et al., who found that the number of viable cells in the TheraCal LC-treated group was lower than in the TheraCal PT-treated group, as determined by an apoptosis/necrosis assay.⁴¹ The cytotoxicity of TheraCal LC has been hypothesized to result from the unpolymerized resin monomers that remain after polymerization.^{42,43} Additionally, some studies have shown that cured TheraCal LC releases specific additives, such as ethyl 4-(dimethylamino)benzoate and camphorquinone.⁴⁴ The primary human pulp fibroblasts exposed to camphorquinone have demonstrated an increase in the production of reactive oxygen species (ROS).^{45,46} This evidence suggests that the light-curing components released from TheraCal LC may contribute to cell death by enhancing the generation of ROS. The absence of mineralization observed in the TheraCal PT group could be attributed to its composition. According to the manufacturer's datasheet, TheraCal PT is a resin-modified calcium silicate cement composed of poly(ethylene glycol) dimethacrylate (PEGDMA) (10–30%) and bisphenol A-glycidyl methacrylate (Bis-GMA) (5–10%). However, the datasheet does not explicitly mention the presence of calcium in its formulation.⁴⁷

Pulpal fibroblasts have been shown to play a significant role in the initiation of inflammatory responses.⁴⁸ In addition, pro-inflammatory cytokines such as VEGF and IL-6, as well as complement fragments C3a and C5a, have been reported to promote the recruitment and activation of cells within an inflammatory microenvironment.^{49,50} Consistent with these findings, the results of the present study demonstrated that MTA and TheraCal LC induced higher levels of VEGF and IL-6 release as compared to the TheraCal PT and control groups. Similarly, TheraCal LC has been reported to increase the secretion of VEGF and IL-6 from pulpal fibroblasts *in vitro*.⁵¹

Although numerous studies have investigated the biological characteristics and biocompatibility of calcium silicate-based cements, including those evaluated in the present study, the rapid introduction of new materials to the market necessitates the continuous and updated biological as well as chemical-mechanical profiling of each formulation prior to clinical application. This highlights

the importance and relevance of animal studies as an initial approach for evaluating novel materials. However, these findings should be interpreted with caution, as the performance of the tested materials may be influenced by several extrinsic factors under clinical conditions.

Conclusions

The findings of the present study demonstrated that TheraCal PT exhibited superior biocompatibility in vivo in comparison with NeoPUTTY (MTA) and TheraCal LC. Therefore, TheraCal PT may be considered a promising material for direct pulp capping. Nevertheless, further studies are recommended to evaluate the additional properties of these materials before their widespread clinical application.

Ethics approval and consent to participate

According to the guidance and approval of the Institutional Animal Care and Use Committee of Cairo University (CU-IACUC), this experiment was conducted in the animal house of the Faculty of Medicine, Cairo University, Giza, Egypt, in accordance with the ARRIVE guidelines for in vivo animal research.

Data availability

The datasets supporting the findings of the current study, including the supplementary material, are available from the corresponding author on reasonable request.

Consent for publication

Not applicable.

Use of AI and AI-assisted technologies

Not applicable.

ORCID iDs

Dina Rady  <https://orcid.org/0000-0002-9672-6935>
 Sara El Moshy  <https://orcid.org/0000-0002-2860-8523>
 Yasmin Mohamed Yousry  <https://orcid.org/0000-0003-3372-5019>
 Mohamed Ramadan  <https://orcid.org/0000-0002-5090-2243>
 Israa Ahmed Radwan  <https://orcid.org/0000-0001-8262-5941>

References

- Shitie A, Addis R, Tilahun A, Negash W. Prevalence of dental caries and its associated factors among primary school children in Ethiopia. *Int J Dent.* 2021;2021:6637196. doi:10.1155/2021/6637196
- Karimi M. Importance of preserving deciduous teeth in childhood. *SAODS.* 2020;3(12):1–5. <https://saods.net/wp-content/uploads/SAODS/PDF-Data/2020/Volume-3-Issue-12/SAODS-03-0189.pdf> Accessed April 1, 2023.
- Kratunova E, Silva D. Pulp therapy for primary and immature permanent teeth: An overview. *Gen Dent.* 2018;66(6):30–38. PMID:30444704.
- Al Tuwirqi AA, El Ashiry EA, Alzahrani AY, Bamashmous N, Bakhsh TA. Tomographic evaluation of the internal adaptation for recent calcium silicate-based pulp capping materials in primary teeth. *Biomed Res Int.* 2021;2021:5523145. doi:10.1155/2021/5523145
- Rajasekharan S, Martens LC, Vandenbulcke J, Jacquet W, Bottenberg P, Cauwels RG. Efficacy of three different pulpotomy agents in primary molars: A randomized control trial. *Int Endod J.* 2017;50(3):215–228. doi:10.1111/iej.12619
- Kim JR, Nosrat A, Fouad AF. Interfacial characteristics of Biodentine and MTA with dentine in simulated body fluid. *J Dent.* 2015;43(2):241–247. doi:10.1016/j.jdent.2014.11.004
- Parirokh M, Torabinejad M. Mineral trioxide aggregate: A comprehensive literature review – Part III: Clinical applications, drawbacks, and mechanism of action. *J Endod.* 2010;36(3):400–413. doi:10.1016/j.joen.2009.09.009
- Cannon M, Gerodias N, Viera A, Percinoto C, Jurado R. Primate pulpal healing after exposure and TheraCal application. *J Clin Pediatr Dent.* 2014;38(4):333–337. doi:10.17796/jcpd.38.4.m585322121536q71
- Gandolfi MG, Siboni F, Botero T, Bossù M, Riccitiello F, Prati C. Calcium silicate and calcium hydroxide materials for pulp capping: Biointeractivity, porosity, solubility and bioactivity of current formulations. *J Appl Biomater Funct Mater.* 2015;13(1):43–60. doi:10.5301/jabfm.5000201
- Arandi NZ, Rabi T. TheraCal LC: From biochemical and bioactive properties to clinical applications. *Int J Dent.* 2018;2018:3484653. doi:10.1155/2018/3484653
- Sanz JL, Soler-Doria A, López-García S, et al. Comparative biological properties and mineralization potential of 3 endodontic materials for vital pulp therapy: Theracal PT, Theracal LC, and Biodentine on human dental pulp stem cells. *J Endod.* 2021;47(12):1896–1906. doi:10.1016/j.joen.2021.08.001
- Marciano MA, Hungaro Duarte MA, Camilleri J. Dental discoloration caused by bismuth oxide in MTA in the presence of sodium hypochlorite. *Clin Oral Investig.* 2015;19(9):2201–2209. doi:10.1007/s00784-015-1466-8
- Sak Mortaş E. Evaluation of the biocompatibility of a light-cured pulp-coating material in the subcutaneous tissue of rats [in Turkish]. Specialization thesis. Karadeniz Technical University, Faculty of Dentistry, Department of Restorative Dentistry; 2016. <https://tez.yok.gov.tr/UlusalTezMerkezi/tezDetay.jsp?id=Veoda9hGcEmVtMn8GRhcFA&no=nzTcFTYBiZaOOnpDhycmLw>. Accessed April 1, 2023.
- Faul F, Erdfelder E, Lang AG, Buchner A. G*Power 3: A flexible statistical power analysis program for the social, behavioral, and biomedical sciences. *Behav Res Methods.* 2007;39(2):175–191. doi:10.3758/bf03193146
- Hulsart-Billström G, Stelzl C, Procter P, et al. In vivo safety assessment of a bio-inspired bone adhesive. *J Mater Sci Mater Med.* 2020;31(2):24. doi:10.1007/s10856-020-6362-3
- Schneider CA, Rasband WS, Eliceiri KW. NIH Image to ImageJ: 25 years of image analysis. *Nat Methods.* 2012;9(7):671–675. doi:10.1038/nmeth.2089
- Da Fonseca TS, Da Silva GF, Tanomaru-Filho M, Sasso-Cerri E, Guerreiro-Tanomaru JM, Cerri PS. In vivo evaluation of the inflammatory response and IL-6 immunoreaction promoted by Biodentine and MTA Angelus. *Int Endod J.* 2016;49(2):145–153. doi:10.1111/iej.12435
- Saraiva JA, Da Fonseca TS, Da Silva GF, et al. Reduced interleukin-6 immunoreaction and birefringent collagen formation indicate that MTA Plus and MTA Fillapex are biocompatible. *Biomed Mater.* 2018;13(3):035002. doi:10.1088/1748-605X/aaa1f5
- Delfino MM, Guerreiro-Tanomaru JM, Tanomaru-Filho M, Sasso-Cerri E, Cerri PS. Immunoinflammatory response and bioactive potential of GuttaFlow bioseal and MTA Fillapex in the rat subcutaneous tissue. *Sci Rep.* 2020;10(1):7173. doi:10.1038/s41598-020-64041-0
- Yaltirik M, Ozbas H, Bilgic B, Issever H. Reactions of connective tissue to mineral trioxide aggregate and amalgam. *J Endod.* 2004;30(2):95–99. doi:10.1097/00004770-200402000-00008
- Zhang W, Peng B. Tissue reactions after subcutaneous and intraosseous implantation of iRoot SP, MTA and AH Plus. *Dent Mater J.* 2015;34(6):774–780. doi:10.4012/dmj.2014-271

22. Mena-Álvarez J, Rico-Romano C, Gutiérrez-Ortega C, Arias-Sanz P, Castro-Urda J. A comparative study of biocompatibility in rat connective tissue of a new mineral trioxide compound (Theracal) versus MTA and a bioactive G3 glass. *J Clin Med*. 2021;10(12):2536. doi:10.3390/jcm10122536
23. Chen Y, Yu Q, Xu CB. A convenient method for quantifying collagen fibers in atherosclerotic lesions by ImageJ software. *Int J Clin Exp Med*. 2017;10(10):14904–14910. <https://e-century.us/files/ijcem/10/10/ijcem0059973.pdf>. Accessed April 1, 2023.
24. Poggio C, Ceci M, Beltrami R, Dagna A, Colombo M, Chiesa M. Biocompatibility of a new pulp capping cement. *Ann Stomatol (Roma)*. 2014;5(2):69–76. PMID:25002921. PMCID:PMC4071365.
25. Murray PE, Godoy CG, Godoy FG. How is the biocompatibility of dental biomaterials evaluated? *Med Oral Patol Oral Cir Bucal*. 2007;12(3):E258–E266. PMID:17468726.
26. Gomes Moura CC, Cunha TC, Crema VO, Dechichi P, Gabrielli Biffi JC. A study on biocompatibility of three endodontic sealers: Intensity and duration of tissue irritation. *Iran Endod J*. 2014;9(2):137–143. PMID:24688584. PMCID:PMC3961592.
27. Khalil WA, Abunasef SK. Can mineral trioxide aggregate and nanoparticulate EndoSequence root repair material produce injurious effects to rat subcutaneous tissues? *J Endod*. 2015;41(7):1151–1156. doi:10.1016/j.joen.2015.02.034
28. Rady D, Mubarak R, Abdel Moneim RA. Healing capacity of bone marrow mesenchymal stem cells versus platelet-rich fibrin in tibial bone defects of albino rats: An in vivo study. *F1000Res*. 2018;7:1573. doi:10.12688/f1000research.15985.1
29. Silva-Herzog D, Ramirez T, Mora J, et al. Preliminary study of the inflammatory response to subcutaneous implantation of three root canal sealers. *Int Endod J*. 2011;44(5):440–446. doi:10.1111/j.1365-2591.2011.01849.x
30. Zmener O, Guglielmotti MB, Cabrini RL. Biocompatibility of two calcium hydroxide-based endodontic sealers: A quantitative study in the subcutaneous connective tissue of the rat. *J Endod*. 1988;14(5):229–235. doi:10.1016/S0099-2399(88)80175-4
31. Giraud T, Jeanneau C, Rombouts C, Bakhtiar H, Laurent P, About I. Pulp capping materials modulate the balance between inflammation and regeneration. *Dent Mater*. 2019;35(1):24–35. doi:10.1016/j.dental.2018.09.008
32. Shahi S, Rahimi S, Lotfi M, Yavari H, Gaderian A. A comparative study of the biocompatibility of three root-end filling materials in rat connective tissue. *J Endod*. 2006;32(8):776–780. doi:10.1016/j.joen.2006.01.014
33. Koh ET, Torabinejad M, Pitt Ford TR, Brady K, McDonald F. Mineral trioxide aggregate stimulates a biological response in human osteoblasts. *J Biomed Mater Res*. 1997;37(3):432–439. doi:10.1002/(sici)1097-4636(19971205)37:3<432::aid-jbm14>3.0.co;2-d
34. Moretton TR, Brown CE Jr., Legan JJ, Kafrawy AH. Tissue reactions after subcutaneous and intraosseous implantation of mineral trioxide aggregate and ethoxybenzoic acid cement. *J Biomed Mater Res*. 2000;52(3):528–533. doi:10.1002/1097-4636(20001205)52:3<528::aid-jbm11>3.0.co;2-9
35. Sahin N, Saygili S, Akcay M. Clinical, radiographic, and histological evaluation of three different pulp-capping materials in indirect pulp treatment of primary teeth: A randomized clinical trial. *Clin Oral Investig*. 2021;25(6):3945–3955. doi:10.1007/s00784-020-03724-4
36. Camilleri J. Hydration characteristics of Biodentine and Theracal used as pulp capping materials. *Dent Mater*. 2014;30(7):709–715. doi:10.1016/j.dental.2014.03.012
37. Bakhtiar H, Nekoofar MH, Aminishakib P, et al. Human pulp responses to partial pulpotomy treatment with TheraCal as compared with Biodentine and ProRoot MTA: A clinical trial. *J Endod*. 2017;43(11):1786–1791. doi:10.1016/j.joen.2017.06.025
38. Hebling J, Rosetti Lessa FC, Nogueira I, Carvalho RM, Souza Costa CA. Cytotoxicity of resin-based light-cured liners. *Am J Dent*. 2009;22(3):137–142. PMID:19650592.
39. Jeanneau C, Laurent P, Rombouts C, Giraud T, About I. Light-cured tricalcium silicate toxicity to the dental pulp. *J Endod*. 2017;43(12):2074–2080. doi:10.1016/j.joen.2017.07.010
40. Hinata G, Yoshihara K, Han L, Edanami N, Yoshihara N, Okiji T. Bioactivity and biomineralization ability of calcium silicate-based pulp-capping materials after subcutaneous implantation. *Int Endod J*. 2017;50(Suppl 2):e40–e51. doi:10.1111/iej.12802
41. Rodríguez-Lozano FJ, López-García S, García-Bernal D, et al. Cytocompatibility and bioactive properties of the new dual-curing resin-modified calcium silicate-based material for vital pulp therapy. *Clin Oral Investig*. 2021;25(8):5009–5024. doi:10.1007/s00784-021-03811-0
42. Li X, Pedano MS, Li S, et al. Preclinical effectiveness of an experimental tricalcium silicate cement on pulpal repair. *Mater Sci Eng C Mater Biol Appl*. 2020;116:111167. doi:10.1016/j.msec.2020.111167
43. Koutroulis A, Kuehne SA, Cooper PR, Camilleri J. The role of calcium ion release on biocompatibility and antimicrobial properties of hydraulic cements. *Sci Rep*. 2019;9(1):1–10. doi:10.1038/s41598-019-55288-3
44. Nilsen BW, Jensen E, Örtengren U, Michelsen VB. Analysis of organic components in resin-modified pulp capping materials: Critical considerations. *Eur J Oral Sci*. 2017;125(3):183–194. doi:10.1111/eos.12347
45. Atsumi T, Ishihara M, Kadoma Y, Tonosaki K, Fujisawa S. Comparative radical production and cytotoxicity induced by camphorquinone and 9-fluorenone against human pulp fibroblasts. *J Oral Rehabil*. 2004;31(12):1155–1164. doi:10.1111/j.1365-2842.2004.01357.x
46. Engelmann J, Volk J, Leyhausen G, Geurtsen W. ROS formation and glutathione levels in human oral fibroblasts exposed to TEGDMA and camphorquinone. *J Biomed Mater Res B Appl Biomater*. 2005;75(2):272–276. doi:10.1002/jbm.b.30360
47. Elbanna A, Atta D, Sherief DI. In vitro bioactivity of newly introduced dual-cured resin-modified calcium silicate cement. *Dent Res J (Isfahan)*. 2022;19:1. doi:10.4103/1735-3327.336686
48. Ananda N, Ariawan D, Juniantito V. Effects of the *Hydnophytum formicarum* plant extract on collagen density, angiogenesis, wound length, and re-epithelialization in wound healing: Experimental study on rats. *Dent Med Probl*. 2022;59(1):67–73. doi:10.17219/dmp/140208
49. Kim I, Moon SO, Kim SH, Kim HJ, Koh YS, Koh GY. Vascular endothelial growth factor expression of intercellular adhesion molecule 1 (ICAM-1), vascular cell adhesion molecule 1 (VCAM-1), and E-selectin through nuclear factor-kappa B activation in endothelial cells. *J Biol Chem*. 2001;276(10):7614–7620. doi:10.1074/jbc.M009705200
50. Yiğit U, Kirzioğlu FY, Özmen Ö, Uğuz AC. Protective effects of caffeic acid phenethyl ester on the heart in experimental periodontitis against oxidative stress in rats. *Dent Med Probl*. 2021;58(3):335–341. doi:10.17219/dmp/132388
51. Giraud T, Jeanneau C, Bergmann M, Laurent P, About I. Tricalcium silicate capping materials modulate pulp healing and inflammatory activity in vitro. *J Endod*. 2018;44(11):1686–1691. doi:10.1016/j.joen.2018.06.009